RELATIONSHIP BETWEEN LIQUEFACTION POTENTIAL AND ROAD SUBSIDENCE: A CASE STUDY OF THE 2011 OFF THE PACIFIC COAST OF TOHOKU EARTHQUAKE IN URAYASU CITY

Rama Mohan Pokhrel[1], Takashi KIYOTA[2], Kazuhiro KAJIHARA[3]

ABSTRACT: Urayasu City, in Chiba prefecture, Japan, is geologically composed of young reclaimed land. Following the 2011 Off the Pacific Coast of Tohoku Earthquake (M_w=9), tilting of houses, buckling of roads and lifelines cut-off etc., associated with severe liquefaction-induced ground subsidence, were extensively observed in this area. Therefore, a detailed study on the potential for and amount of ground subsidence was essential in such area. In this paper, the variation of road subsidence was studied after severe liquefaction took place during the 2011 earthquake. Randomly distributed boreholes were collected to study the liquefaction potential. Accordingly, geostatistical method of interpolation was applied to attain a spatial variation of liquefaction potential within the study area. Moreover, ground subsidence was estimated by using airborne LiDAR (Light Detection And Ranging) images taken before and after the earthquake, providing the spatial distribution of soil subsidence. Finally, the relationship between liquefaction potential and road subsidence was developed.

Key Words: Reclaimed land, Liquefaction potential, Subsidence, GIS, Road pavement

INTRODUCTION

Soil liquefaction is one of the most serious geotechnical issues related to earthquakes that may induce severe ground subsidence, lateral spreading, tilting of super structures and uplift of light underground structures, especially in a loose sandy deposit. Urayasu City, Chiba Prefecture, Japan, which is geologically composed of newly reclaimed land (the reclamation in this area was completed between 1966 and 1985), suffered severe liquefaction during the 2011 Off the Pacific Coast of Tohoku Earthquake (M_W =9.0). Yasuda et al. (2012) reported that about 85% of Urayasu City was heavily damaged due to the liquefaction. Figure 1 shows a manhole uplifted during liquefaction in Urayasu city.

In Urayasu city, soil dredged from the sea bed was filled to the height of about sea level in the reclamation work. Then, it was covered with hill sand transported from Boso Peninsula (Yasuda et al., 2012). For that reason, the surface soil in Urayasu reclaimed land area was highly prone to liquefaction during the severe 2011 earthquake.

This paper, presents a detailed study for evaluating the spatial distribution of liquefaction potential and soil subsidence in Urayasu City. To do so, 109 boreholes (shown in Figure 2 as red dots) were selected to calculate the liquefaction potential for a peak ground acceleration of 173 gal for

---

[1] JSPS Postdoctoral Research fellow, Institute of Industrial Science, University of Tokyo
[2] Associate Professor, Institute of Industrial Science, University of Tokyo
[3] Undergraduate student, Department of Civil Engineering, Yokohama National University

Motomachi area and 200 gal for Nakamachi and Shinmachi area (Urayasu City, 2012).

Figure 1 Manhole uplifted during the 2011 earthquake in Urayasu City

A geostatistical method of interpolation in a Geographic Information System (GIS) was used to evaluate the spatial distribution of liquefaction potential in the area. This method gives the liquefaction potential value at each point. Similarly, the soil subsidence map of this area was prepared by analyzing Digital Surface Model (DSM) data taken before (2006) and just after (2011) the earthquake. By comparing these maps the relationship between liquefaction potential and ground subsidence was developed. In this paper, the measurement of ground subsidence concentrated on the type of roads to investigate the effectiveness of pavement thickness against road subsidence.
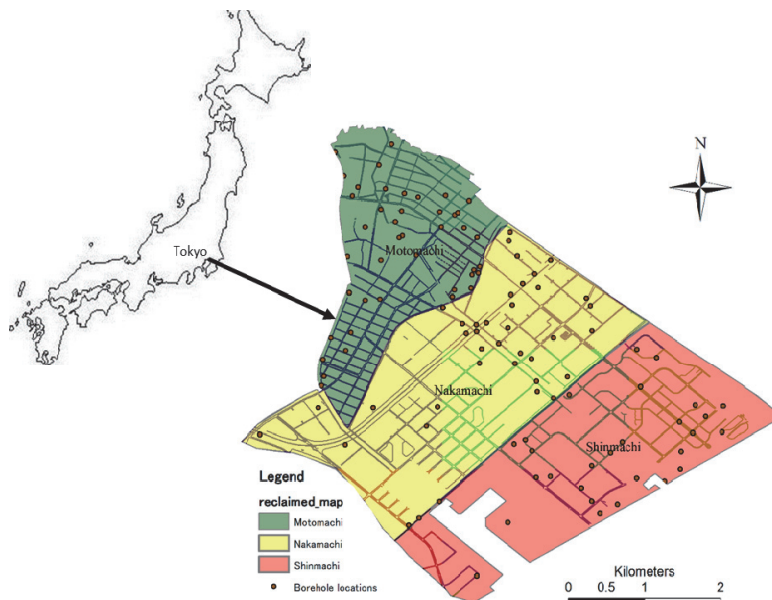

Figure 2 Location of study area with borehole points

METHODOLOGY

Liquefaction potential at borehole

For the liquefaction potential zoning, the main step was the collection and calculation of geotechnical data from boreholes on which the liquefaction resistance factor for a given soil layer was evaluated. In this paper, the liquefaction resistant parameter was evaluated by using Road Bridge manual (2012). BY applying this method, soil liquefaction was estimated based on the test results of standard penetration tests (SPTs). Moreover, the liquefaction potential at each sampled borehole location was quantified by an index called the liquefaction potential index, P_L, defined by Iwasaki et al. (1982). Finally, a database containing the coordinates and liquefaction potential index P_L at each borehole was prepared for GIS analysis and interpolation.

Geostatistics for interpolation

A surface is a continuous field of values that may vary over an infinite number of points and impossible to measure and record the liquefaction potential at every point. Therefore in this study a geostatistical method was used to interpolate the liquefaction potential at unsampled (where borehole data were not available) locations. A kriging method which is an exact and powerful interpolation method in geostatistics was used for interpolation. In kriging, the first step is to examine the data in order to identify the spatial structure, which is often represented by the empirical semivariogram (Isaaks and Srivastava, 1989). A semivariogram is a figure that shows the relationship between semivariance and the distance between all the pairs of available data points, as schematically illustrated in Figure 3. The experimental semivariance for liquefaction potential was calculated using Eqn. 1 (Pokhrel et al. 2012, 2013):

$$\gamma(h) = \frac{1}{2N(h)} \sum_{i=1}^{N(h)} \left(P_L(i) - P_L(i,h) \right)^2 \quad \text{.............. (1)}$$

In the above, $\gamma(h)$ is the estimated value of the semivariance for distance of h; $N(h)$ is the number of experimental pairs separated by h; and $P_L(i)$ and $P_L(i,h)$ are the values of the variables P_L at (i) and (i,h) positions respectively.

Kriging weights the surrounding measured values to derive a prediction for an unsampled location. To estimate the weight value for the surrounding measured locations the experimental semivariogram dots in Figure 3 was constructed from the measured values. These dots give the degree of relationship between points on the surface. The model variogram curve line shown in Figure 3 was fitted for the experimental variogram. In kriging, weights are based not only on the distance between the measured
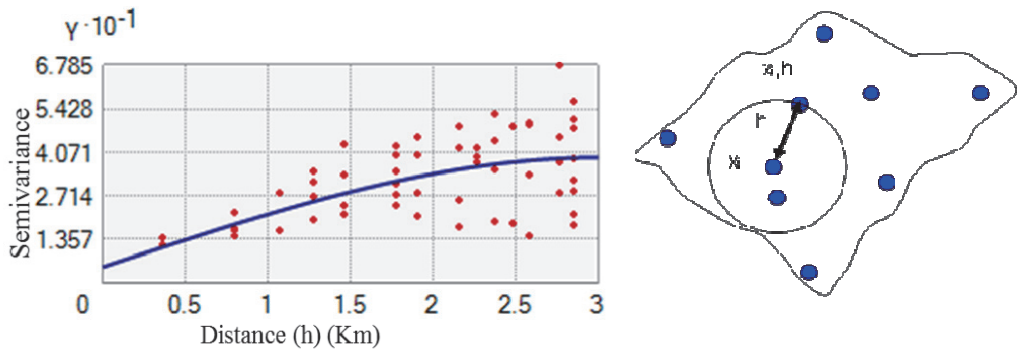

Figure 3 Kriging variogram model

points and the prediction location, but also on the overall spatial relationships of the measured values surrounding the prediction location (i.e. the model variogram, Figure 3).
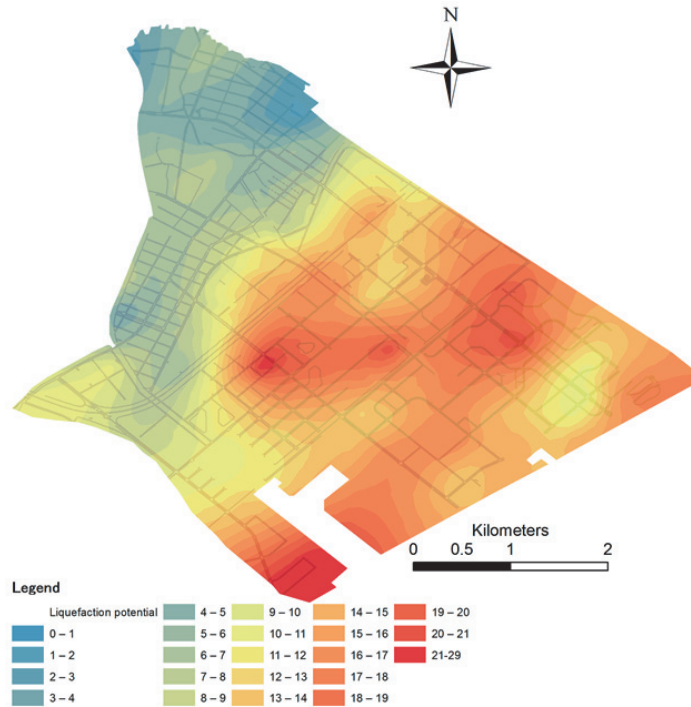

Figure　4　Liquefaction potential distribution map of the Urayasu Area

After considering suitable model for interpolation the liquefaction potential distribution map of the Urayasu City was prepared as shown in Figure 4. This map illustrate that the Nakamachi and Shinmachi areas have high liquefaction potential, but Motomachi area has low liquefaction area. The newly reclaimed area falls on high liquefaction potential zone and the natural alluvial deposit area falls on low liquefaction potential zone. This map was finally used to pick up the liquefaction potential value for the analysis.

Ground subsidence

At the time of 2011 Off the Pacific Coast of Tohoku Earthquake liquefaction- induced soil subsidence was severally observed in the Tokyo bay area especially in Urayasu city. Most of the roads, parks, buildings and embankments subsided. Therefore, in this study, an attempt was made to find the relationship between liquefaction potential and subsidence. For this purpose the subsidence map prepared by Konagai et al. 2013 shown in Figure 5 was used for the study area. Konagai et al. (2013) obtained this map by analysing LiDAR images before (2006) and after (2011) the Off the Pacific Coast of Tohoku Earthquake. The colour intensity represents the amount of change in elevation. To estimate ground subsidence at a specific point, the required area was zoomed out as the area X in Figure 5. A line about 100 m length was drawn on the road as shown in zoomed area. This section of road was then divided into ten parts. In each 10 m interval a profile was drawn across the road and the elevation value on 2011 and 2006 was extracted from the subsidence map and plotted as in Figure 6. The starting and ending points of each profile is indicated by the arrows in Figure 5.
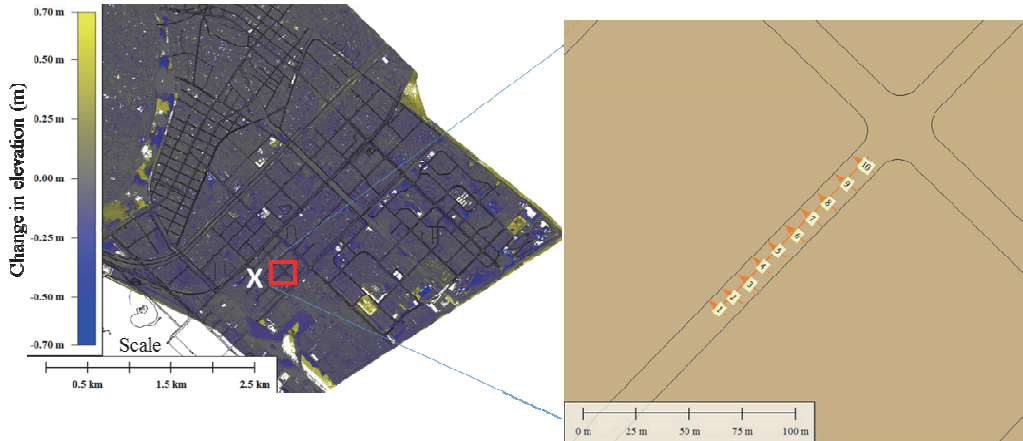
Figure 5　Ground subsidence map of Urayasu area (Konagai et al., 2013)

The elevation value taken at each point from the Digital Surface Model (DSM) data of 2011 and 2006 is plotted in Figure 6. It is observed that the elevation measured in 2011 was lower than that measured in 2006. The difference in elevation is increasing towards arrow pointing direction, which indicates the tilting of roads by differential settlement. The difference in elevation value from two curves are plotted in Figure 7. The average elevation was taken for particular point for this curve. The road subsidence data was evaluated for different types of road mainly highway, city road, and community road. These roads were constructed with different thickness of the road pavement and roadbed.
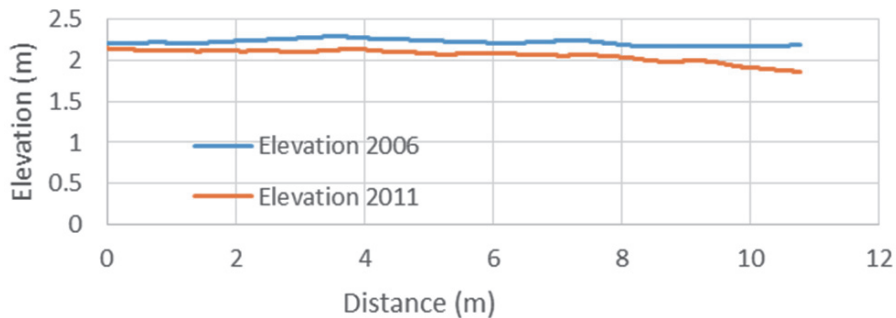

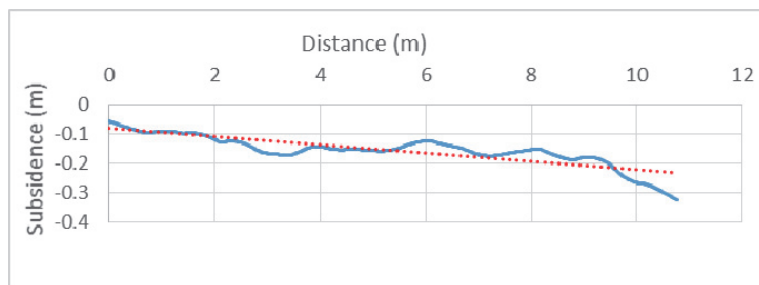**Figure 6**　Profile across the road along line 1 in Figure 6 shows elevation of ground surface on 2006 and 2011

Figure 7　A ground settlement curve in a particular section of the road

RESULTS

The spatial variation of liquefaction potential map, prepared as described in above section, is shown in Figure 8 (a). Most of the areas are zoned as high liquefaction potential areas. The reclaimed part of the city has very high liquefaction potential. The city area with thick natural alluvial soil deposits is zoned as low liquefaction. During 2011 earthquake most of Urayasu area experienced severe liquefaction, but there was very few evidence of liquefaction observed in the natural soil as shown in Figure 8(b) prepared by the Committee for countermeasure technology and investigation of liquefaction in Urayasu City (2012). This figure shows the post-earthquake inspection made by committee. In the reclaimed area many buildings were significantly damaged as shown in Figure 8(b) but few roads were damaged in the natural deposited area. The degree of road damage and sewer pipeline damage are also shown in the map.

Figure 8(b) was also used to validate the methodology used for preparation of liquefaction potential map in Figure 8(a). The comparison of these maps shows that the observation of buildings with liquefaction damage are fall on the high liquefaction potential area in the Figure 8(a), except for the points in the blue circle area. Such exception may be due possibly to the availability of only few sampled boreholes (Figure 2), as well as the obtained liquefaction potential for the borehole within the blue circle shows low liquefaction potential.

In this study, Figure 8 (a) was used to determine the liquefaction potential value for a particular point, similarly, the road subsidence values for corresponding points were determined from Figure 5. The green and pink dots in Figure 8(a) are the locations where liquefaction potential and corresponding road subsidence value were extracted. The subsidence at the green dots in Figure 8(a) were extracted by Suyama (2013).
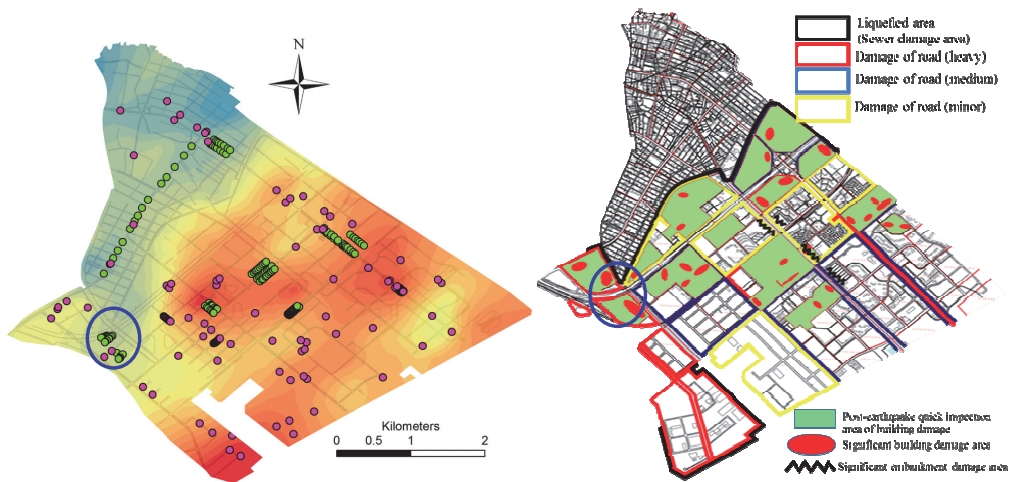

Figure 8 (a) Liquefaction potential distribution map (The green and pink points represent the location of the result observation), b) Outline of liquefaction damage (Committee for countermeasures 2012)

Figure 9 shows the relationship between liquefaction potential and ground subsidence. The larger the liquefaction potential, the larger the ground subsidence. This study also focused on the effectiveness of the thickness of road pavement and roadbed on the settlement. As explained in Figure 9 the thickness of the road subgrade were different for the different roads. All the roads were classified as three classes based on the thickness of the road pavement and roadbed. The National highway has pavement and roadbed thicker than 115 cm. The main road or city road has subgrade ranging between 65 cm and 90 cm. The third class is for residential roads having road pavement and roadbed thinner
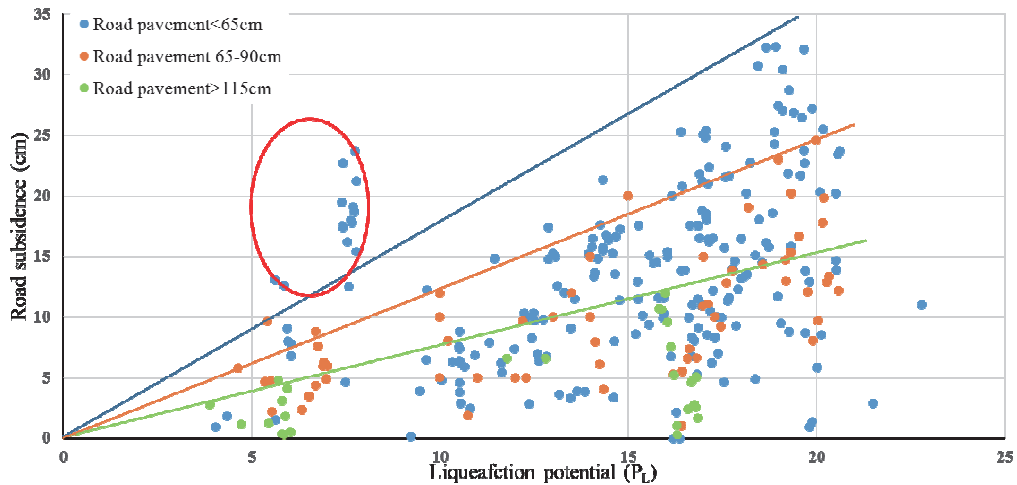
Figure 9   Relationship between liquefaction potential and road subsidence

than 65 cm. As shown in Figure 9 all the roads show increasing trend of settlement with liquefaction potential. Though the road subsidence increases with increasing liquefaction potential, the amount of settlement for different roads has different trend. The thicker the road pavement and roadbed, the lower the settlement. In Figure 9, some of the data plotted in the red circle show large road subsidence in the lower liquefaction potential. The data set obtained in Figure 9 were compared with the map shown in Figure 8(a). The locations of these exceptional points were picked up within the blue circle in Figure 8(a). Figure 9 shows that the enclosed area in blue circle significantly liquefied during the 2011 Off the Pacific Coast of Tohoku Earthquake. Therefore, the ground settlement value was also large. For the interpolated liquefaction map, this area has less sampled borehole data which may cause such inaccurate result.

SUMMARY

Most of the reclaimed area of Urayasu City suffered severe liquefaction in the 2011 off the Pacific Coast of Tohoku Earthquake. Sand boiling, tilting of structures, uplift of light underground structures, lifeline cut-off etc. were the most common problems associated with the liquefaction. Among these problems, ground subsidence was likely the main issue. The spatial distribution of liquefaction potential map of Urayasu City was prepared by using a geostatistical method over 109 boreholes and was correlated with ground subsidence extracted from DSM by Konagai et al. (2013). The result shows that there is a linear relationship between the liquefaction potential and the road subsidence. Such relationship shows that the thicker the road pavement and roadbed, the lower the subsidence of road. The old natural deposits area with very low liquefaction potential has minor subsidence.

ACKNOWLEDGEMENTS

REFERENCES

Committee for countermeasure technology and investigation of liquefaction in Urayasu city, 2012. *A report of the Committee for countermeasure technology and investigation of liquefaction in Urayasu city*. Pp 23. (Japanese)

Isaaks, E.H., Srivastava, R.M., 1989. An Introduction to Applied Geostatistics. Oxford University press, Oxford, 561pp.

Iwasaki, T., Tokida, K., Tatsuoka, F., Watanabe, S., Yasuda, S., and Sato, H., 1982. Microzonation for soil liquefaction potential using simplified methods. Proceedings of 3rd International Earthquake Microzonation Conference, Seattle, 1319-1330.

Japan road association 2012. Seismic designed specifications for Highway bridge volume V.

Konagai, K., kiyota, T., Suyama, S., Asakura, T., Shibuya, K., Eto, C., 2013. Maps of soil subsidence for Tokyo bay shore areas liquefied in the March 11th, 2011 off the pacific Coast of Tohoku Earthquake. Soil Dynamics and Earthquake Engineering, Vol.53, pp 240-253.

Pokhrel, R.M., Kuwano, J., Tachibana, S. 2012. Geostatistical analysis for spatial evaluation of liquefaction potential in Saitama City. Lowland Technology International, vol. 14, No.1, pp. 45-51.

Pokhrel, R.M., Kuwano, J., Tachibana, S. 2013. A kriging method of interpolation used to map liquefaction potential over alluvial ground. Engineering Geology, Vol. 152, pp. 26-37.

Suyama, S. 2013. Soil subsidence map of the liquefied Tokyo bay area and its exploitation in multiple factor analyses of liquefaction impact. A master thesis submitted to department of Civil Engineering, University of Tokyo (In Japanese).

Urayasu City, 2012. Data compiled by the Technical Committee on measures against Liquefaction URL http://www.city.urayasu.chiba.jp/menu11324.html (in Japanese).

Yasuda, S., Harada, K., Ishikawa, K, Kanemaru, Y. (2012) Characteristics of liquefaction in Tokyo Bay area by the 2011 Great East Japan Earthquake. Soils and Foundations, Vol. 52(5): 793-810.